LETTER

doi:10.1038/nature10655

The oxidation state of Hadean magmas and implications for early Earth's atmosphere

Dustin Trail[1,2], E. Bruce Watson[1,2] & Nicholas D. Tailby[1,2]

Magmatic outgassing of volatiles from Earth's interior probably played a critical part in determining the composition of the earliest atmosphere, more than 4,000 million years (Myr) ago[1]. Given an elemental inventory of hydrogen, carbon, nitrogen, oxygen and sulphur, the identity of molecular species in gaseous volcanic emanations depends critically on the pressure (fugacity) of oxygen. Reduced melts having oxygen fugacities close to that defined by the iron–wüstite buffer would yield volatile species such as CH_4, H_2, H_2S, NH_3 and CO, whereas melts close to the fayalite–magnetite–quartz buffer would be similar to present-day conditions and would be dominated by H_2O, CO_2, SO_2 and N_2 (refs 1–4). Direct constraints on the oxidation state of terrestrial magmas before 3,850 Myr before present (that is, the Hadean eon) are tenuous because the rock record is sparse or absent. Samples from this earliest period of Earth's history are limited to igneous detrital zircons that pre-date the known rock record, with ages approaching ~4,400 Myr (refs 5–8). Here we report a redox-sensitive calibration to determine the oxidation state of Hadean magmatic melts that is based on the incorporation of cerium into zircon crystals. We find that the melts have average oxygen fugacities that are consistent with an oxidation state defined by the fayalite–magnetite–quartz buffer, similar to present-day conditions. Moreover, selected Hadean zircons (having chemical characteristics consistent with crystallization specifically from mantle-derived melts) suggest oxygen fugacities similar to those of Archaean and present-day mantle-derived lavas[2–4,9,10] as early as ~4,350 Myr before present. These results suggest that outgassing of Earth's interior later than ~200 Myr into the history of Solar System formation would not have resulted in a reducing atmosphere.

The oxygen fugacity (f_{O_2}) of a magma influences mineral saturation, element partitioning and the molecular speciation of gases exsolved on eruption[1–4]. Traditionally, the oxidation state of ancient eruptives is assessed by measuring Fe^{3+}/Fe^{2+} values of unaltered glass samples[11]. For less pristine ancient samples, researchers rely on changes in crystal–liquid partitioning versus f_{O_2} for heterovalent transition elements such as V and Cr that are generally regarded as immobile during rock alteration[2,3]. Studies of this nature have provided consistent lines of evidence that the upper mantle reached its present-day oxidation state by 3.6 Gyr ago and perhaps as early as 3.9 Gyr (ref. 3). Whereas the final oxidation state of a glass or mineral reflects that of the parent magma, subsequent metamorphism or alteration at Earth's surface may reset the primary redox equilibria. Preservation of the redox state of the most primitive Hadean magmas therefore requires a physically and chemically robust repository. Fortunately, zircon is an exceptionally durable mineral that retains primary chemistry for most elements and isotopes from the time of igneous crystallization[12], and zircon crystals are the only known terrestrial solids dating from the first 500 Myr of Earth history. Zircon thus presents a unique opportunity to evaluate the oxidation state of terrestrial melts before the Archaean if the partitioning of a variable-valence cation into zircon can be characterized as a function of f_{O_2}.

Here we report a calibration to determine the oxidation state of a magmatic melt based on the incorporation of cerium (Ce) into zircon. Cerium is unique among elements that partition into zircon (and among the rare-earth elements, REEs) in that it can exist in melts as either Ce^{4+} or Ce^{3+}. The magnitude of Ce enrichment in zircon depends on the Ce^{4+}/Ce^{3+} ratio of the medium from which it crystallizes. Because Ce^{4+} is vastly more compatible than Ce^{3+} in zircon, more-oxidized melts will yield higher Ce contents in the mineral. To explore the details of Ce uptake, zircons were grown in a piston cylinder apparatus at a pressure of 1 GPa and at temperatures of 900–1,300 °C from hydrous silicate melts (~72 wt% SiO_2) doped with lanthanum (La), Ce and praseodymium (Pr) (with and without phosphorus). Lanthanum and Pr were included as 'bracketing' elements because these exist only as 3+ ions, and partition coefficients for zircon trivalent REEs are known to monotonically increase from La to lutetium (Lu) (ref. 13); by convention, partition coefficients are expressed as the crystal/melt concentration ratio, $D_{REE}^{zrc/melt}$ (here zrc indicates zircon, the crystal concerned). This systematic behaviour provides a convenient reference for natural zircon to characterize the relative enrichment of Ce in zircon, relative to other REEs, with changes in f_{O_2}. This is expressed as a 'Ce anomaly', $(Ce/Ce^*)_D$, and is calculated in the following manner:

$$\left(\frac{Ce}{Ce^*}\right)_D = \frac{D_{Ce}^{zrc/melt}}{\sqrt{D_{La}^{zrc/melt} \times D_{Pr}^{zrc/melt}}} \quad (1)$$

where $D_{Ce}^{zrc/melt}$ is the combined partition coefficient of Ce^{4+} and Ce^{3+} in zircon, and $D_{La}^{zrc/melt}$ and $D_{Pr}^{zrc/melt}$ are respectively the partition coefficients for trivalent La and Pr. The denominator on the right hand side (equal to Ce*) is the interpolated value for the Ce^{3+} partition coefficient based on the partition coefficients of bracketing elements La and Pr. Accordingly, if $(Ce/Ce^*)_D \approx 1$, then Ce^{4+} must have been effectively absent in the melt at the time of zircon crystallization.

The Ce^{4+}/Ce^{3+} ratio of the melt was varied by imposing different oxygen fugacities on the experimental charges, broadly corresponding to the range observed in terrestrial magmas. The change in element partitioning in response to differences in f_{O_2} was then measured in synthesized zircon populations and melts using an electron microprobe. The results show that Ce anomalies are inversely related to temperature (Fig. 1) and can be expressed by the following empirical equation:

$$\ln\left(\frac{Ce}{Ce^*}\right)_D = (0.1156 \pm 0.0050) \times \ln(f_{O_2}) + \frac{13{,}860 \pm 708}{T} - 6.125 \pm 0.484 \quad (2)$$

where f_{O_2} is the oxygen fugacity and T is temperature in K (T can be estimated for natural samples using the Ti-in-zircon thermometer[7]).

Phosphorus substitution for silicon is known to compensate the charge imbalance accompanying the entry of trivalent REEs into

[1]Department of Earth and Environmental Sciences, Rensselaer Polytechnic Institute, Troy, New York 12180, USA. [2]New York Center for Astrobiology, Rensselaer Polytechnic Institute, Troy, New York 12180, USA.

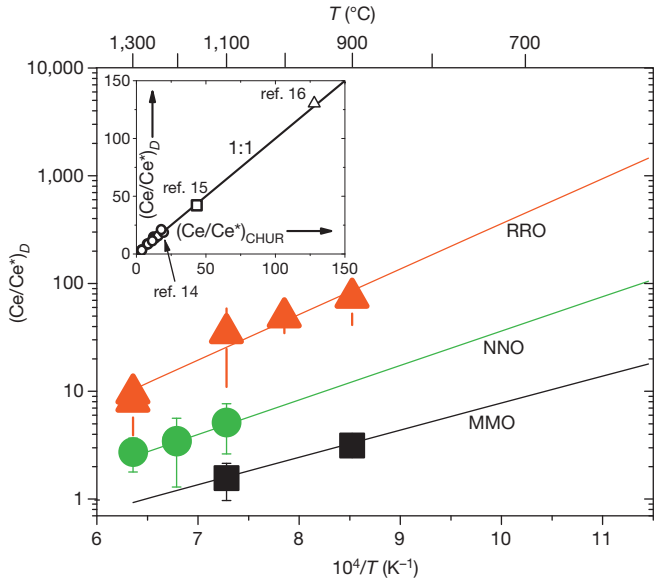

Figure 1 | Experimental calibration, relating melt oxygen fugacity to zircon Ce anomalies and temperature. On average, six zircons and five glasses were analysed for each of the 11 experiments. (Two experiments each at 1,300 °C/RRO and 1,200 °C/NNO yield virtually identical Ce anomalies and plot on top of each other.) The Ru–RuO_2 (RRO) buffer defines an oxygen fugacity (f_{O_2}) that is ~1 log unit greater than that of the magnetite–haematite (MH) buffer at ~1,000 °C, Ni–NiO (NNO) is ~0.8 log units greater than FMQ, and the Mo–MoO_2 (MMO) buffer is nearly identical to IW (<0.5 log units) at all temperatures. The curves drawn are fits to the data according to equation (2). Inset, Ce anomalies from natural zircon–melt partitioning studies[14–16] (reference numbers are shown); calculated partition coefficients (subscript 'D') are compared to those normalized to chondrite (subscript 'CHUR'). Error bars, 1σ.

zircon, but the addition of 0.15–0.8 wt% P_2O_5 to three experiments did not lead to differences in $(Ce/Ce^*)_D$. In addition, two experiments resulted in the saturation of light-REE-bearing phases allanite and monazite, but showed no detectable change in $(Ce/Ce^*)_D$ of zircon. These observations suggest that the calibration is unaffected by the presence of light-REE phases or the P content of the melt.

Before applying equation (2) to natural samples, it is important to note that in most natural settings $(Ce/Ce^*)_D$ cannot be calculated because the REE concentration of the melt at the time of zircon saturation is unknown. As an alternative, Ce anomalies are often calculated by normalizing to the chondritic uniform reservoir (CHUR), in which case the relationship between $(Ce/Ce^*)_D$ and $(Ce/Ce^*)_{CHUR}$ must be established. Plotting $(Ce/Ce^*)_D$ versus $(Ce/Ce^*)_{CHUR}$ for natural zircon–melt partitioning studies[14–16] demonstrates a near perfect 1:1 correlation (Fig. 1 inset), suggesting that $(Ce/Ce^*)_D \approx (Ce/Ce^*)_{CHUR}$ is a reasonable assumption for out-of-context zircons. In other words, the magnitude of the Ce anomaly will be independent of the concentration of trace elements in the melt as long as the light REEs are not fractionated relative to one another.

If the assumptions outlined above are valid, then zircon data[6,17] give an average f_{O_2} of 0.5 log units below the value defined by the fayalite–magnetite–quartz (FMQ) buffer (±2.3 log units) for Hadean melts, excluding the single outlier that plots well below the iron–wüstite (IW) buffer curve (Fig. 2). Lunar zircon source melts yield a calculated oxygen fugacity at IW (±1.3 log units), which is within error of previous estimates from lunar rocks and minerals[18]. Also note that lunar zircon Ce anomalies show a clear inverse relationship with temperature, in agreement with the prediction of equation (2). There is no correlation between temperature or age versus difference from the IW buffer for lunar zircons, though the Hadean zircons exhibit a weak trend towards more reducing conditions with lower crystallization temperatures.

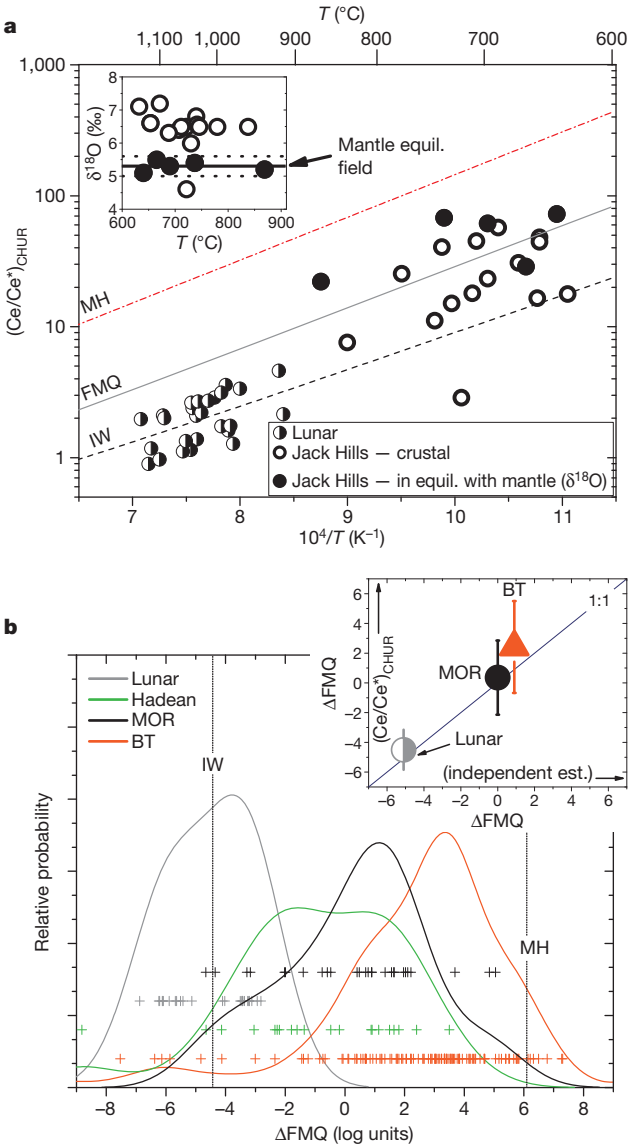

Figure 2 | Oxygen fugacity and oxygen isotope plots for natural samples using the experimental calibration. a, Main panel; $(Ce/Ce^*)_{CHUR}$ versus $1/T$ for Jack Hills Hadean and lunar zircons with MH, FMQ and IW buffer curves (equation (2)). Inset, $\delta^{18}O$ versus temperature. Filled symbols, crystals that have $\delta^{18}O$ values in the mantle equilibrium field for zircon ($n = 5$)[20] (inset), samples shown by open symbols yield $\delta^{18}O$ values more akin to a crustal origin ($n = 15$). The open and filled symbols in the main panel and the inset are from the same samples. **b**, Oxygen fugacity probability distribution plots for lunar ($n = 27$)[19], Hadean ($n = 20$)[6,17], mantle-derived mid-ocean ridge (MOR) residual liquids ($n = 27$)[22–24] and Bishop Tuff (BT) magma-chamber ($n = 120$)[30] zircons. Values of f_{O_2} are given as difference from FMQ in log units (ΔFMQ). The coloured symbols correspond to calculated f_{O_2} values from individual zircons. Zircon host melts have calculated f_{O_2} values for the aforementioned samples of IW (±1.3), FMQ − 0.5 (±2.3), FMQ + 0.4 (±2.6), FMQ + 2.4 (±3.1), respectively. The calculated f_{O_2} values are in agreement with independent f_{O_2} estimates for BT[30], MOR[10] and the Moon[18] (inset). The errors are in log units and they represent the standard deviations of f_{O_2} values from individual sample sets.

Accepting for the moment that terrestrial Hadean zircons probably crystallized under relatively oxidizing conditions (when compared to lunar zircons), the remaining question is whether they truly reflect the prevailing f_{O_2} of Earth's early mantle, which was the dominant source of volcanic emanations forming the early atmosphere. Lunar zircons did in fact crystallize from mantle-derived melts—specifically the residual liquid fraction of the lunar magma ocean[19]. Most terrestrial Hadean zircons, on the other hand, crystallized from crust-derived

felsic melts, as indicated by multiple geochemical signatures[6,8,9]. Oxygen isotopes, for example, demonstrate that the vast majority of terrestrial Hadean zircons fall outside the zircon mantle equilibrium field ($\delta^{18}O_{VSMOW} = 5.3 \pm 0.3$ ‰ (1σ))[5,20], which is a strong argument for the input of supracrustal material into the source melts. Moreover, most zircon crystallization temperatures are consistent with formation in water-saturated or near-water-saturated melts[7,8].

Conclusions about the oxidation state of the Hadean mantle based on zircons of crustal affinity are admittedly indirect. However, a subset of the Hadean zircon population does appear to be mantle-derived. (We note that direct partial melts of the mantle cannot crystallize zircon, but the fractionation products (residuals) of such melts do eventually saturate in zircon[21].) Five of the Hadean crystals have $\delta^{18}O$ values that fall within the mantle equilibrium field, which has been shown to be constant (±0.2‰) for the past 4.4 Gyr (ref. 20). If these $\delta^{18}O$ values are primary, then these zircons crystallized from uncontaminated, mantle-derived melts that did not interact with the hydrosphere. The five zircons in the $\delta^{18}O$ mantle equilibrium field—including two crystals with U–Pb ages approaching 4,400 Myr—give a calculated oxygen fugacity of FMQ + 1.4 (±2) (Fig. 3). As a comparison, zircons crystallized from residual liquids of present-day mantle-derived mid-ocean ridge basalts[22–24] yield calculated f_{O_2} values of FMQ + 0.4 (±2.6), which agrees with estimates of the oxidation state of the upper mantle[10]. This also implies that the redox conditions in residual, zircon-saturated liquids of present-day mid-ocean ridge systems did not undergo significant changes in f_{O_2} (relative to the buffer curve) along the liquid line of descent from basalt. This is also consistent with observations from lunar zircons. Finally, we note that Martian basalts (for example, shergottite meteorite Dar al Gani 476) exhibiting little or no interaction with a crustal component are only about 1 log unit higher than the estimated f_{O_2} of the upper mantle[25]. Furthermore, calculated oxygen fugacities from the same meteorite are all within a log unit of the average (FMQ − 2.5), even though phases cover a crystallization range of >300 °C.

As in all studies in which mantle f_{O_2} is estimated from mantle-derived glasses or minerals[3,9], it is important to emphasize that the calculated f_{O_2} may not directly reflect that of the mantle source region. We note, however, that mantle-derived Hadean zircons would have had to crystallize from residual melts that underwent ~4 log units of change in f_{O_2} to be reconcilable with mantle source regions in equilibrium with the IW buffer. At present and in the Archaean, relative f_{O_2} changes along magmatic liquid lines of descent are broadly of the order of ~1 log unit[4,10,26,27]. If the evolution of Hadean melts was similarly constrained, then our results imply that the mantle reached its present-day oxidation state ~4,350 Myr ago (Fig. 3). This interpretation is consistent with core formation models calling for physical and chemical isolation from the (upper) mantle ~30 Myr after planet formation[28].

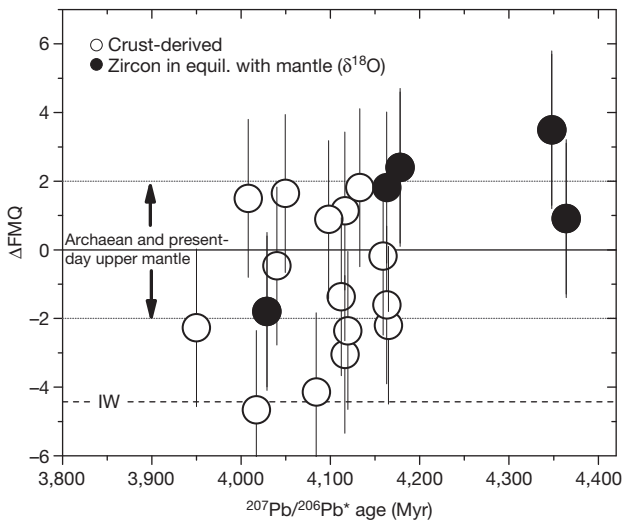

Figure 3 | Oxygen fugacities of Hadean melts plotted against zircon crystallization age. Errors for individual points are based on the standard deviation of the entire data set ($n = 20$; $1\sigma = \pm 2.3$ log units). Zircons with mantle signatures are within error of the estimated oxidation state of the present-day and Archaean upper mantle[3,10,26]. On average, oxygen fugacities are lower for younger zircons, though this trend is not robust given the present data set.

If our deductions regarding the oxidation state of Hadean magmas are correct, then the speciation of gases emanating from the Earth at this time would have been dominated by CO_2, SO_2, H_2O and N_2 (ref. 26). An atmosphere of this composition is known to yield a lower abundance of sugars and especially amino acids and nucleotides[1]. If a highly reduced atmosphere is required for the origin of life, then it may have occurred exceptionally early on our planet. However, pre-4,400-Myr outgassing of H_2 coupled with slow escape[29] may have resulted in an atmosphere out of equilibrium with Earth's interior. Alternatively, a 'late veneer' may have served as a source of pre-biotic molecules. These alternative scenarios notwithstanding, our results offer the first glimpse into the oxidation state of terrestrial magmas before 3,900 Myr ago, and the data presented here open up the possibility of exploring the oxidation state of zircon-bearing rocks throughout the geologic record. This calibration will be especially valuable in the early Archaean or Hadean eons, for which zircon is often the only source of primary chemical information.

METHODS SUMMARY

Starting materials were contained in platinum (Pt) or silver (Ag) capsules, and f_{O_2} was buffered by placing ruthenium and ruthenium dioxide (Ru+RuO_2; RRO) in direct physical contact with the experimental charge or by use of a separate buffer chamber separated by a Pt or silver-palladium (Ag-Pd) membrane (NNO or MMO). Quenched glasses were analysed by electron microprobe, with at least one measurement made at the top and bottom of the capsule to assess melt homogeneity. Synthesized zircons were small (~3–20 μm) and in some cases the glass was dissolved with hydrofluoric acid (HF) and the zircons recovered in order to obtain more accurate measurements.

For the inset plot of Fig. 1, $Pr_x = 2/3(La)_x + 1/3(Nd)_x$ for ref. 14, where x represents a normalized value, either to CHUR or the melt. Ce anomalies for natural zircons[6,19,23–25,30] are calculated in a similar fashion to equation (1) in the text: $(Ce/Ce^*)_{CHUR} = Ce_{CHUR}/(La_{CHUR} \times Pr_{CHUR})^{1/2}$, where La_{CHUR} and so on represents normalization to the chondritic uniform reservoir rather than the melt concentration. Ce anomalies are plotted for Hadean zircons with U–Pb ages that are ≥94% concordant, and with REE+Ti measurements that reflect primary igneous chemistry[5,6,17]. Zircon crystallization temperatures in Fig. 2 are calculated assuming unity Ti-activity[7]; sub-unity Ti activity (for example, ~0.5) results in systematic shifts of all data to higher values of f_{O_2}, though shifts are within error of the standard deviation of each population. Lunar zircons are from Apollo 14 polymict breccias 14304, 14305 and 14321[19] and are normalized to an average f_{O_2} of IW at 700 °C, for direct comparison with the other data in the probability distribution plot of Fig. 2. For the inset of Fig. 2b, average f_{O_2} values calculated from zircon Ce anomalies are plotted against independent estimates from lunar basaltic igneous rocks (IW − 0.6)[18], terrestrial mid-ocean ridge basalts[10] (FMQ), and average oxygen fugacities returned from Bishop Tuff titanomagnetite-ilmenite pairs (NNO)[27].

Full Methods and any associated references are available in the online version of the paper at www.nature.com/nature.

Received 22 March; accepted 6 October 2011.

1. Kasting, J. F. Earth's early atmosphere. *Science* **259,** 920–926 (1993).
2. Canil, D. Vanadium partitioning and the oxidation state of Archaean komatiite magmas. *Nature* **389,** 842–845 (1997).
3. Delano, J. W. Redox history of the Earth's interior since ~3900 Ma: implications for prebiotic molecules. *Orig. Life Evol. Biosph.* **31,** 311–341 (2001).
4. Burgisser, A. & Scaillet, B. Redox evolution of a degassing magma rising to the surface. *Nature* **445,** 194–197 (2007).
5. Cavosie, A. J., Valley, J. W., Wilde, S. A., &. Edinburgh Ion Microprobe Facility. Magmatic $\delta^{18}O$ in 4400–3900 Ma detrital zircons: a record of the alteration and recycling of crust in the early Archean. *Earth Planet. Sci. Lett.* **235,** 663–681 (2005).
6. Cavosie, A. J., Valley, J. W., Wilde, S. A., &. Edinburgh Ion Microprobe Facility. Correlated microanalysis of zircon: trace element, $\delta^{18}O$, and U-Th-Pb isotopic constraints on the igneous origin of complex 3900 Ma detrital grains. *Geochim. Cosmochim. Acta* **69,** 637–648 (2006).

7. Watson, E. B. & Harrison, T. M. New thermometer reveals minimum melting conditions on earliest Earth. *Science* **308,** 841–844 (2005).
8. Hopkins, M., Harrison, T. M. & Manning, C. M. Low heat flow inferred from >4 Gyr zircons suggests Hadean plate boundary interactions. *Nature* **456,** 493–496 (2008).
9. Berry, A. J. Danyushevsky, L. V., O'Neill, H. St. C., Newville, M. & Sutton, S. R. Oxidation state of iron in komatiitic melt inclusions indicates hot Archaean mantle. *Nature* **455,** 960–963 (2008).
10. Mallmann, G. & O'Neill, H. St. C. The crystal/melt partitioning of V during mantle melting as a function of oxygen fugacity compared with some other elements (Al, P, Ca, Sc,Ti, Cr, Fe, Ga,Y, Zr and Nb). *J. Petrol.* **50,** 1765–1794 (2009).
11. Carmichael, I. S. E. & Ghiorso, M. S. The effect of oxygen fugacity on the redox state of natural liquids and their crystallizing phases. *Rev. Mineral.* **24,** 191–212 (1990).
12. Cherniak, D. J., Hanchar, J. M. & Watson, E. B. Rare-earth diffusion in zircon. *Chem. Geol.* **134,** 289–301 (1997).
13. Rubatto, D. & Hermann, J. Experimental zircon/melt and zircon/garnet trace element partitioning and implications for the geochronology of crustal rocks. *Chem. Geol.* **241,** 38–61 (2007).
14. Thomas, J. B., Bodnar, R. J., Shimizu, N. & Sinha, A. K. Determination of zircon/melt trace element partition coefficients from SIMS analysis of melt inclusions in zircon. *Geochim. Cosmochim. Acta* **66,** 2887–2901 (2002).
15. Hinton, R. W. & Upton, B. G. J. The chemistry of zircon: variations within and between large crystals from syenite and alkali basalt xenoliths. *Geochim. Cosmochim. Acta* **55,** 3287–3302 (1991).
16. Sano, Y., Terada, K. & Fukuoka, T. High mass resolution ion microprobe analysis of rare earth elements in silicate glass, apatite and zircon: lack of matrix dependency. *Chem. Geol.* **184,** 217–230 (2002).
17. Fu, B. *et al.* Ti-in-zircon thermometry: applications and limitations. *Contrib. Mineral. Petrol.* **156,** 197–215 (2008).
18. Sato, M., Hickling, N. L. & McLane, J. E. in *Proc. Fourth Lunar Science Conference* Vol. 1 (ed. Grose, W. A.) 1061–1079 (Geochim Cosmochim Acta Suppl. 4, Pergamon, 1973).
19. Taylor, D. J., McKeegan, K. D. & Harrison, T. M. Lu–Hf zircon evidence for rapid lunar differentiation. *Earth Planet. Sci. Lett.* **279,** 157–164 (2009).
20. Valley, J. W. *et al.* 4.4 billion years of crustal maturation: oxygen isotope ratios of magmatic zircon. *Contrib. Mineral. Petrol.* **150,** 561–580 (2005).
21. Watson, E. B. & Harrison, T. M. Zircon saturation revisited: temperature and composition effects in a variety of crustal magma types. *Earth Planet. Sci. Lett.* **64,** 295–304 (1983).
22. Coogan, L. A. & Hinton, R. W. Do trace element compositions of detrital zircons require Hadean continental crust? *Geology* **34,** 633–636 (2006).
23. Schmitt, A. K. *et al.* Rapid cooling rates at an active mid-ocean ridge from zircon thermochronology. *Earth Planet. Sci. Lett.* **302,** 349–358 (2011).
24. Cavosie, A. J., Kita, N. K. & Valley, J. W. Primitive oxygen-isotope ratio recorded in magmatic zircon from the Mid-Atlantic Ridge. *Am. Mineral.* **94,** 926–934 (2009).
25. Herd, C. D. K., Borg, L. E. & Jones, J. H. Oxygen fugacity and geochemical variations in the Martian basalts: implications for Martian basalt petrogenesis and the oxidation state of the upper mantle of Mars. *Geochim. Cosmochim. Acta* **66,** 2025–2036 (2002).
26. Frost, D. J. & McCammon, C. A. The redox state of Earth's mantle. *Annu. Rev. Earth Planet. Sci.* **36,** 389–420 (2008).
27. Hildreth, W. & Wilson, C. J. N. Compositional zoning of the Bishop Tuff. *J. Petrol.* **48,** 951–999 (2007).
28. Kleine, T., Munker, C., Mezger, K. & Palme, H. Rapid accretion and early core formation on asteroids and the terrestrial planets from Hf-W chronometry. *Nature* **418,** 952–955 (2002).
29. Tian, F., Toon, O. B., Pavlov, A. A. & De Stereck, H. A hydrogen-rich early Earth atmosphere. *Science* **308,** 1014–1017 (2005).
30. Reid, M. R., Vazquez, J. A. & Schmitt, A. K. Zircon-scale insights into the history of a Supervolcano, Bishop Tuff, Long Valley, California, with implications for the Ti-in-zircon geothermometer. *Contrib. Mineral. Petrol.* **161,** 293–311 (2011).

Supplementary Information is linked to the online version of the paper at www.nature.com/nature.

Acknowledgements This work was supported by the NASA Astrobiology Institute (grant no. NNA09DA80A to The New York Center for Astrobiology).

Author Contributions E.B.W. identified the importance of investigating redox sensitive elements in zircon. D.T. designed the experiments and took measurements. D.T. wrote the manuscript and interpreted the data with significant contributions from E.B.W. and N.D.T.

Author Information Reprints and permissions information is available at www.nature.com/reprints. The authors declare no competing financial interests. Readers are welcome to comment on the online version of this article at www.nature.com/nature. Correspondence and requests for materials should be addressed to D.T. (traild@rpi.edu).

METHODS

Zircons were synthesized in silicate melts with water added as silicic acid, gibbsite, $Zr(OH)_4 \pm H_2O$ (ref. 31). Experiments run from 1,000 to 1,300 °C contained ~8–10 wt% H_2O and those run at 900 °C contained 12 wt% H_2O, which was found to aid zircon synthesis at lower temperatures. Saturation of other REE-bearing phases was generally avoided by doping melt compositions with progressively lower REE concentrations for lower-temperature experiments. (Starting compositions can be found in Supplementary Table 1.)

The pressure cell used here is similar to that described in ref. 32. Capsules made of either Ag (900 °C) or Pt (1,000–1,300 °C) were pressure sealed with Pt or Ag-Pd gaskets respectively to ensure a water tight seal. The highest oxygen fugacity imposed on the experimental charges was comprised of a 9:1 mixture of RuO_2:Ru added with the starting silicate mix into the capsule. This is a common buffering technique because RuO_2 is virtually insoluble in silicate melts. At run termination, the buffer was inspected to ensure the presence of RuO_2 and Ru, and that both phases were in clear chemical communication with the glass and synthesized zircons. Experiments buffered at NNO or MMO contained a chamber external to the experiment that contained the metal, oxide and H_2O. For experiments run at 1,000–1,300°C, Pt capsules were surrounded by either a Mo or an oxidized Ni holder, while those at 900 °C were contained within a thick-walled Ag capsule, and the buffer was separated by a thin sheet of 30Pd-70Ag metal. These experiments are buffered by the permeability of H_2 through Pt or 30Pd-70Ag; that is, fixing the hydrogen fugacity (f_{H_2})at MMO or NNO buffers the f_{O_2} in a similar matter to that described in ref. 33. A diagram of the experimental set-ups can be found in Supplementary Fig. 1.

Synthesized zircons (~3–20 μm) were analysed using the Rensselaer Polytechnic Institute Cameca SX100 electron microprobe. All elements were calibrated on standards for every electron microprobe session (accelerating voltage, 15 kV). The only interference was the slight overlap of the La L_β peak with the L_α line of Pr. This was removed by synthesizing a melt with 0–2 wt% of La_2O_3 so that the contribution of La L_β to Pr L_α counts could then be subtracted out. The major elements of the melts were analysed with a beam current of 10 nA and a 40–60 μm spot size, and trace elements with a 50 nA, 30 μm spot size (analysed glass compositions can be found in Supplementary Table 2).

Zircons were analysed with a focused beam and depending on crystal size, electron microprobe currents ranged from 20 to 200 nA; synthetic REE-phosphates and zircon were used as standards. Aluminium was used as a monitor for secondary fluorescence and in some cases after the melt was analysed, it was dissolved in HF, so that the recovered zircon fraction could be analysed. Single acquisition times as long as 1,000 s were used for the high-temperature experiments especially, which yielded the lowest partition coefficients. For some zircons, multiple acquisitions were made on the same crystal to accumulate additional counts. In order to increase the counting time for the La L_α peak, essentially 3 of the 5 spectrometers (the counting time on one spectrometer was split between La and Ce) were devoted to simultaneous peak counting (large pentaerythritol (LPET) crystal), and accumulated totals were used to obtain a concentration. Another spectrometer was used for Si K_α, Zr L_α, Al K_α (thallium acid phthalate (TAP)) while the final was used for Pr (large lithium fluoride (LLIF)). Under this protocol, the detection limits for La, Ce and Pr are ~30, ~100 and ~80 p.p.m., respectively. Because of the very low counts on some unknowns, zircons were synthesized without REEs and measured under the same protocols to test for trace interferences on the peak and background positions. Zircon concentrations along with individual grains in glass and epoxy matrix are shown for comparison in Supplementary Table 3. The partition coefficients used to construct Fig. 2 of the main text are provided in Supplementary Table 4.

All data used to create Figs 2 and 3 are included in Supplementary Table 5. Two criteria were considered when applying our calibration to Hadean grains. First, it is known that Hadean zircons may record multiple episodes of growth over their >4 Gyr history, meaning that grains may be heterogeneous in age and chemistry. Our calibration is applied to zircons for which the following determinations were performed on the same location on the crystal: (1) U/Pb age, (2) oxygen isotope, (3) magmatic REE concentrations and (4) temperature (Ti-thermometry) data. Correlated geochemical data for the first three items can be found in ref. 6. These data are then compared with the analysis location of Ti-thermometry results published in ref. 17. Grains were further considered pristine if U/Pb concordance (that is, $[^{206}Pb^*/^{238}U$ age$]/[^{207}Pb/^{206}Pb^*$ age$] \times 100$, expressed as percentage concordance) was, on average, 94%. The oxygen fugacities for these pristine grains are plotted in Fig. 2, and the data used are included in Supplementary Table 5. All lunar zircons with REE and Ti data from ref. 19 are included; grains reported in that study are ~94% concordant or better. The ~800,000-year-old zircons from the Bishop Tuff and those collected near present-day active mid-ocean ridges are all assumed to be pristine; all data with Ti-thermometry and REE data are included in Fig. 2b. Ce anomalies are calculated from La, Ce and Pr concentrations using equation (1) in the text but with chondrite normalized values; results agree with those reported in the above studies with the exception of ref. 30.

31. Trail, D. Watson, E. B. & Thomas, J. B. The incorporation of OH into zircon. *Am. Mineral.* **96,** 60–67 (2011).
32. Watson, E. B., Wark, D. A. & Thomas, J. B. Crystallization thermometers for zircon and rutile. *Contrib. Mineral. Petrol.* **151,** 413–433 (2006).
33. Ayers, J. C., Brenan, J. B., Watson, E. B., Wark, D. A. & Minarik, W. G. A new capsule technique for hydrothermal experiments using the piston cylinder apparatus. *Am. Mineral.* **77,** 1080–1086 (1992).